(12 He

NRL Report 8180

AD A053449

Hydrophone Preamplifier Optimization

Prediction of Hydrophone Self-Noise by a Noise Model

A. C. Tims

Transducer Branch
Underwater Sound Reference Division
Orlando, Florida

March 17, 1978

NAVAL RESEARCH LABORATORY
Washington, D.C.

SECURITY CLASSIFICATION OF THIS PAGE (When Data Entered)

REPORT DOCUMENTATION PAGE

READ INSTRUCTIONS BEFORE COMPLETING FORM

1. REPORT NUMBER
14 NRL [redacted] 8180

2. GOVT ACCESSION NO.

3. RECIPIENT'S CATALOG NUMBER

4. TITLE (and Subtitle)
HYDROPHONE PREAMPLIFIER OPTIMIZATION,

Prediction of Hydrophone Self-Noise by a Noise Model

5. TYPE OF REPORT & PERIOD COVERED
Interim report on a continuing NRL Problem

6. PERFORMING ORG. REPORT NUMBER

7. AUTHOR(s)
10 Allan C. Tims

8. CONTRACT OR GRANT NUMBER(s)

9. PERFORMING ORGANIZATION NAME AND ADDRESS
Naval Research Laboratory
Underwater Sound Reference Division
P.O. Box 8337, Orlando, FL 32856

10. PROGRAM ELEMENT, PROJECT, TASK AREA & WORK UNIT NUMBERS
PE: 62711N
Project/Task: ZF11-121-003
Problem: 82S02-31.701

11. CONTROLLING OFFICE NAME AND ADDRESS
Department of the Navy
Office of Naval Research
Arlington, VA 22217

12. REPORT DATE
March 17, 1978

13. NUMBER OF PAGES
12 22 p.

14. MONITORING AGENCY NAME & ADDRESS (if different from Controlling Office)

15. SECURITY CLASS. (of this report)
UNCLASSIFIED

15a. DECLASSIFICATION/DOWNGRADING SCHEDULE

16. DISTRIBUTION STATEMENT (of this Report)
Approved for public release; distribution unlimited. 9 Interim rept.,

12 17 Mar 78

17. DISTRIBUTION STATEMENT (of the abstract entered in Block 20, if different from Report)
16 F11121 17 ZF11121003

18. SUPPLEMENTARY NOTES

19. KEY WORDS (Continue on reverse side if necessary and identify by block number)
Hydrophone preamplifier
Electrical noise
Preamplifier
Self-noise

20. ABSTRACT (Continue on reverse side if necessary and identify by block number)
This report presents analysis of the self-noise which determines the threshold pressure level in hydrophone designs. The noise present in the acoustic sensor, coupling network, and preamplifier input stage are represented by an equivalent circuit noise model. A model provides an effective method to predict in advance of sensor-preamplifier construction the noise levels expected for a specific design.

DD FORM 1 JAN 73 1473 EDITION OF 1 NOV 65 IS OBSOLETE
S/N 0102-LF-014-6601

SECURITY CLASSIFICATION OF THIS PAGE (When Data Entered)

251 150

CONTENTS

HYDROPHONE PREAMPLIFIER OPTIMIZATION
PREDICTION OF HYDROPHONE SELF-NOISE BY A NOISE MODEL

INTRODUCTION

A hydrophone consists of two well-defined components — the acoustic sensor element and the preamplifier. For noise-measuring hydrophones the design focal points are high acoustic sensitivity for the sensor element and low self-noise from the preamplifier [1]. When the requirements of omnidirectionality and broad bandwith are added to these, the sensor element can become so small that inadequate impedance loading is provided for the preamplifier, resulting in prohibitive self-noise.

Self-noise is a result of the preamplifier electronic-noise mechanisms and the thermal-noise contribution of the sensor element. Most of the noise originates at the input stage of the preamplifier; the acoustic element actively contributes thermal noise proportional to its impedance loading on the input.

This report presents noise modeling and circuit analysis of the noise which limits the threshold pressure level in any hydrophone design. Using noise analysis, a designer can establish minimum noise levels and understand the limiting factors for a specific design, without actual construction and after-the-fact noise measurements [2].

THERMAL NOISE

According to the well-known Johnson-Nyquist equation, electrons in every conductor are in random motion. This motion is temperature dependent, and the mean-square thermal-noise voltage is

$$E_t^2 = 4kTR\Delta f,$$

where

k = Boltzmann's constant, 1.38×10^{-23} J/K,

T = temperature of the conductor in K,

R = resistance, or real part of the conductor's impedance,

and

Δf = noise bandwidth in Hz.

Figure 1 shows an equivalent circuit for thermal noise, represented by a noise-voltage generator in series with a noiseless resistance. According to Norton's theorem, the series circuit of Fig. 1 can be replaced by a constant-current generator in parallel with a resistance as in Fig. 2.

Manuscript submitted November 1, 1977.

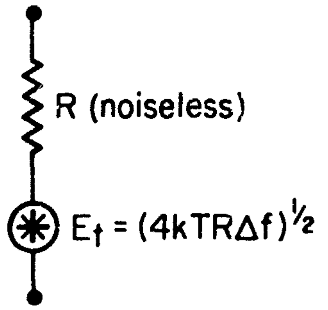

Fig. 1 – Equivalent circuit for thermal-noise-voltage generator

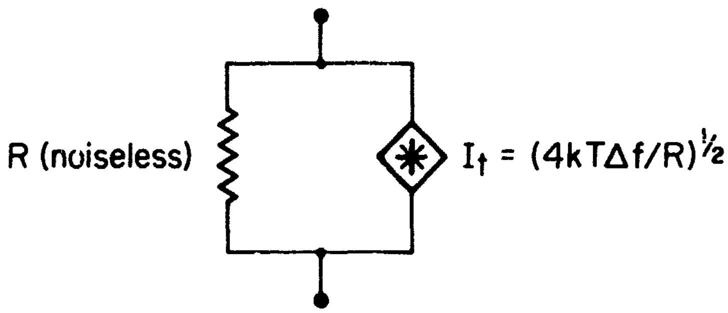

Fig. 2 – Equivalent circuit for thermal-noise-current generator

NOISE-CIRCUIT ANALYSIS CONSIDERATIONS

When several noise sources are acting simultaneously in a linear network, the total noise is the sum of the sources acting independently, with the other voltage sources short-circuited and the other current sources open-circuited. The contributions from each source are added, so that the magnitude of the noise is increased by the contribution from each source.

Equivalent-noise generators represent a large number of component frequencies with a random distribution of amplitudes and phases. When there is no relationship between instantaneous values from independent generators, their voltages are uncorrelated. However, if their voltages are equal and fully correlated, the maximum error caused by the assumption of independence is only 3 dB. If the voltages are partially correlated, or if one is of much greater amplitude than the other, the error is less. Thus one can assume the correlation to be zero, with little error.

THE NOISE MODEL

To perform a noise analysis of a hydrophone system, one represents the components of the hydrophone sensor and preamplifier by a noise model. Since the input noise is determined by the sensor impedance and by the first transistor stage of the preamplifier, modeling is confined to this area. To further simplify analysis, one assumes the sensor to be small in comparison with the wavelength, the mechanical losses very small, and the impedance almost entirely reactive.

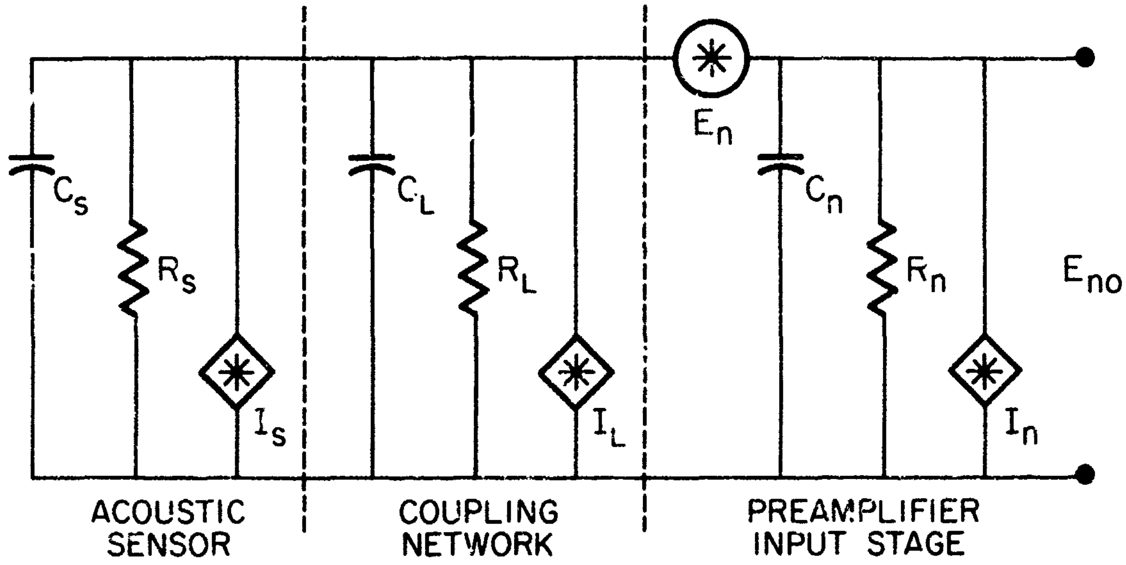

Fig. 3 – Noise model of hydrophone

The schematic diagram of Fig. 3 shows the $E_n - I_n$ equivalent-noise representation for a hydrophone electronic system, with its three distinctive sections: the acoustic sensor element, the coupling network, and the preamplifier input stage. In Fig. 3,

C_s = capacitance of the acoustic sensor element,

C_L = shunt capacitance across C_s due to inner electrode capacitance and dielectric changes caused by the acoustic coupling medium of the hydrophone sensor head,

C_n = preamplifier input capacitance,

R_s = resistance of the sensor,

R_L = resistance across R_s caused by the volume resistance of the acoustic coupling medium ($R_L = R_H R_s / R_s - R_H$, where R_H is the measured terminal resistance of the oilfilled hydrophone head),

R_n = preamplifier input resistance,

E_n = input-transistor midband noise voltage,

I_n = input-transistor midband noise current,

I_s = sensor rms equivalent-noise-current generator,

and

I_L = coupling network rms equivalent-noise current.

To find the equivalent input noise E_{ni}, the total output noise E_{no} is calculated using Kirchhoff's laws. The equivalent input noise is the output noise E_{no} divided by the system gain K, where the system gain can be either a voltage, current, or impedance transfer function as needed.

In Fig. 3 the mean-square output noise voltage is

$$E_{no}^2 = E_n^2 + (\mathrm{Re}Z_T)^2 I_T^2, \tag{1}$$

where

$$(\mathrm{Re}Z_T)^2 = R_T^2/(1 + \omega^2 R_T^2 C_T^2) \tag{2}$$

is the square of the real part of the impedance, with

$$R_T = 1/(1/R_s + 1/R_L + 1/R_n) \tag{3}$$

and

$$C_T = C_s + C_L + C_n. \tag{4}$$

Also, in (1),

$$I_T^2 = I_s^2 + I_L^2 + I_n^2, \tag{5}$$

where

$$I_s^2 = 4kT/R_s \tag{6}$$

and

$$I_L^2 = 4kT/R_L. \tag{7}$$

This leads to

$$E_{no}^2 = E_n^2 + I_T^2 [R_T^2/(1 + \omega^2 R_T^2 C_T^2)]. \tag{8}$$

E_{no}^2 is the total noise at the output of the system, in V^2/Hz, with the amplifier gain unity. If the amplifier gain is greater than unity, the total noise is simply the product of the unity E_{no}^2 term and the gain A, since amplification does not change the signal-to-noise ratio.

To compute the voltage transfer function K, consider the circuit of Fig. 4, a simplified circuit of Fig. 3, where C_s and R_T are as previously defined, $C_D = C_T - C_s$, V_n and V_o are the input and output voltages of the network, and i_1 and i_2 the appropriate loop currents. Then

$$\begin{bmatrix} (R_T + 1/j\omega C_s) & -R_T \\ -R_T & (R_T + 1/j\omega C_D) \end{bmatrix} \begin{bmatrix} i_1 \\ i_2 \end{bmatrix} = \begin{bmatrix} V_n \\ 0 \end{bmatrix}, \tag{9}$$

$$i_2 = V_n R_T/\Delta, \tag{10}$$

and

$$V_o = i_2 (Z_o) = i_2/j\omega C_D. \tag{11}$$

Thus

$$V_o/V_n = \frac{R_T/j\omega C_D}{(R_T + 1/j\omega C_s)(R_T + 1/j\omega C_D) - R_T^2} = K \tag{12}$$

and

$$K = \frac{R_T}{R_T[(C_s + C_D)/C_s] - j/\omega C_s}. \tag{13}$$

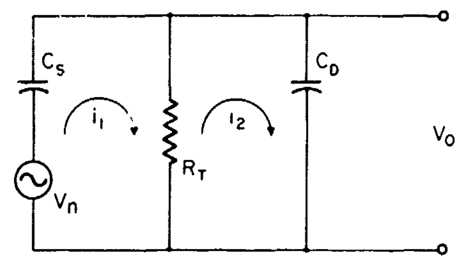

Fig. 4 – Simplified circuit of Fig. 3 with input voltage source V_n and output voltage V_O

Since $C_T \approx C_D + C_s$, then

$$K = \omega C_s R_T / (\omega C_T R_T - j); \tag{14}$$

the modulus of (14) squared becomes K^2, where

$$K^2 = \omega^2 C_s^2 R_T^2 / (\omega^2 C_T^2 R_T^2 + 1). \tag{15}$$

The mean-square equivalent input noise is

$$E_{ni}^2 = E_{no}^2 / K^2. \tag{16}$$

Thus

$$E_{ni}^2 = E_{no}^2 [(1 + \omega^2 C_T^2 R_T^2)/\omega^2 R_T^2 C_s^2] + (I_s^2 + I_L^2 + I_n^2)/\omega^2 C_s^2. \tag{17}$$

In the circuit analysis, E_n and I_n are given as midband values. In order for the noise voltage and current to be representative of device-noise characteristics, a shaping factor is applied for each case, as a function of frequency. For noise voltage, the factor is

$$E_n^2(f) = E_n^2 [(1 + F_1/f) + (f/F_2)^2], \tag{18}$$

and for the noise current,

$$I_n^2(f) = I_n^2 [(1 + F_3/f) + (f/F_4)^2], \tag{19}$$

where F_1 and F_2 are low- and high-frequency E_n noise corners, F_3 and F_4 are low- and high-frequency I_n noise corners, and f is the frequency of interest [2, p.142].

A Bodie plot of (18) and (19) is shown in Fig. 5. At frequencies below F_1 and F_3 the noise rises 3 dB/octave to characterize the $1/f$ noise mechanisms of the input transistor; at midband the noise is independent of frequency; and at F_2 and F_4 the noise rises 6 dB/octave, because of transistor gain rolloff.

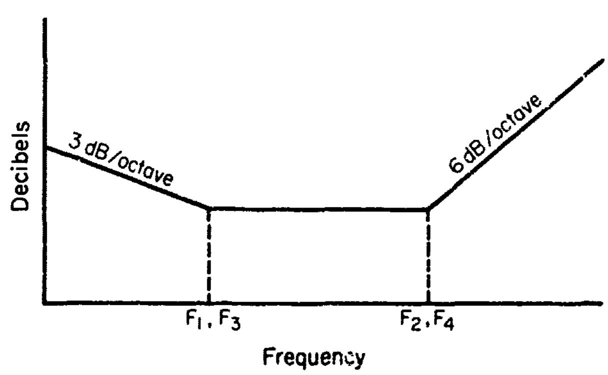

Fig. 5 – Shaping factor, noise characteristics

A program was written for the Hewlett-Packard 9810A calculator which solves (8), (15), (17), (18), and (19). Values for resistance, capacitance, noise current, noise voltage, and frequency can be readily substituted to quickly determine their effect on the output noise, the input noise, or the transfer function. (Appendix A describes the effects of varying the values of components.)

Figure 6 shows the equivalent noise pressure curve for a USRD type H56 standard-reference hydrophone, which was calculated from the measured noise voltage. Also shown is the theoretical equivalent noise pressure, derived as outlined in this report. Knudsen's sea-state-zero curve is indicated as a reference.

The equivalent noise pressure is computed by using E_{no} and free-field voltage sensitivity M_e of the hydrophone. If M_e represents the hydrophone sensitivity at the output of the preamplifier, then

$$P_{en} = E_{no} - M_e, \tag{20}$$

where the units are decibels referred to 1 μPa.

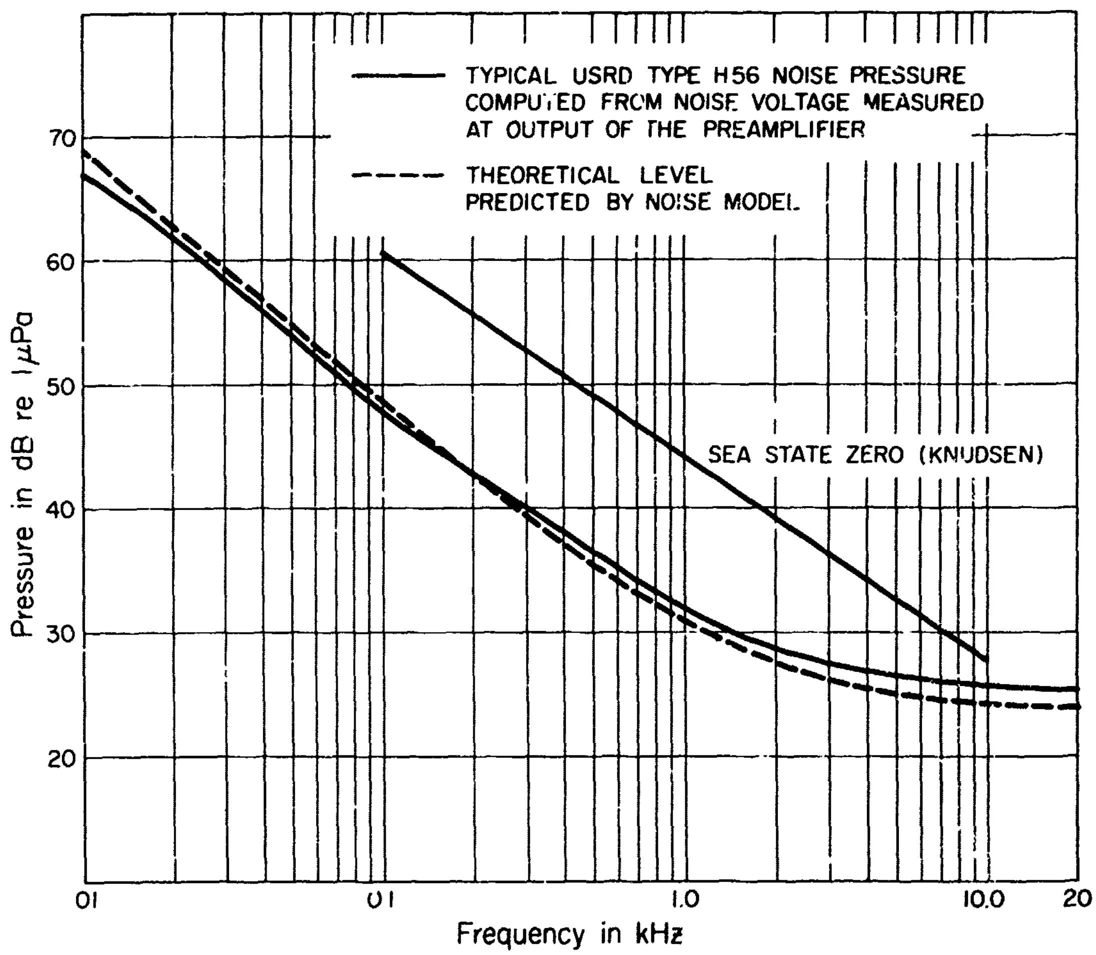

Fig. 6 – Equivalent noise pressure

CONCLUSION

Often a black-art approach is used to design a low-noise hydrophone. However, noise modeling provides an effective method to predict in advance of actual circuit or sensor construction the self-noise level to be expected from a specific design. With the aid of a minicomputer or a good programmable calculator, analysis can be quick and accurate. In most cases, the noise model need not be more complex than presented herein.

ACKNOWLEDGMENTS

The author thanks Theodore A. Henriquez and Craig K. Brown of the USRD and Dr. Hans Fuehrer of Rollins College, Winter Park, Florida, for their impetus, expert guidance, and review. Portions of this report have been submitted to the School of Continuing Studies, Rollins College, for the Bachelor of Science degree.

REFERENCES

1. R.W. Timme, R.L. Davidson, and A.C. Tims, "Expendable Hydrophone for Sonobuoy Application," NRL Report 7644, 17 Sept. 1973.
2. C.D. Motchenbacher and F.C. Fitchen, *Low-Noise Electronic Design*, John Wiley, New York, 1973.

BIBLIOGRAPHY (Electronic Noise and Low-Noise Hydrophone Design)

I.D. Groves, Jr., "Low-Noise Hydrophone for All Underwater Ocean Environments," Eighth International Congress on Acoustics, London, July 1974, Vol. 2.

I.D. Groves, Jr., "A Hydrophone for Measuring Acoustic Ambient Noise in the Ocean at Low Frequencies" (USRD Type H62), NRL Report 7738, 15 Apr. 1974.

T.A. Henriquez, "An Extended-Range Hydrophone for Measuring Ocean Noise," J. Acoust. Soc. Amer. **52**, 1450-1455 (1972).

W.A. Rheinfelder, *Design of Low-Noise Transistor Input Circuits*, Hayden, New York, 1964.

B. Watson, "Audio-Frequency Noise Characteristics of Junction FETs," Application Note AN 74-4, Siliconix Incorporated, Santa Clara, Calif., Aug. 1974.

A. Van der Ziel, *Noise*, Prentice-Hall, New York, 1954.

Appendix A

THE EFFECTS OF CIRCUIT VALUES ON SELF-NOISE

The following figures present the resulting noise levels when one component value of the noise model is varied while the others are held constant. Some curves are of equivalent input noise E_{ni}, and others are of equivalent output noise E_{no}; tabulation of the transfer function K is also presented. The curves are a plot of dB versus frequency; therefore,

$$E_{ni}\ (\mathrm{dB}) = E_{no}\ (\mathrm{dB}) - K\ (\mathrm{dB}). \tag{A1}$$

For the noise model in Fig. A1, the constant values for the components are given in Table A1.

Table A1 – Constant Values for the Noise-Model Circuit of Fig. A1

C_s	C_L	C_n	R_s	R_L	R_n	I_n	I_s	I_L	E_n
100 pF	10 pF	20 pF	1 GΩ	1 GΩ	1 GΩ	1 fA/$\sqrt{\mathrm{Hz}}$	$\sqrt{4KT/R_s}$ A/$\sqrt{\mathrm{Hz}}$	$\sqrt{4KT/R_L}$ A/$\sqrt{\mathrm{Hz}}$	1 nV/$\sqrt{\mathrm{Hz}}$

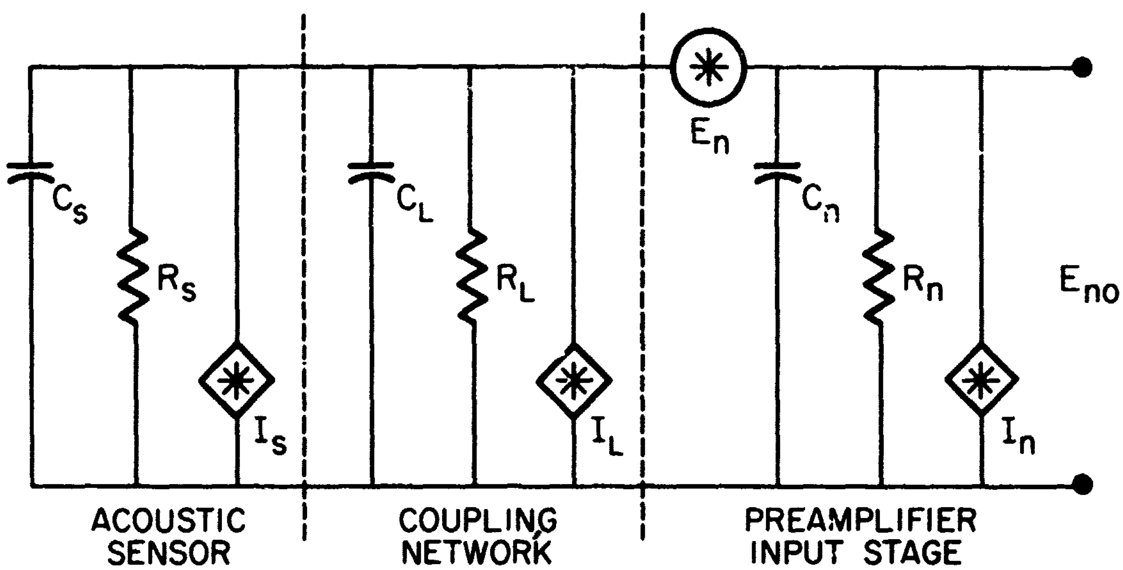

Fig. A1 – Noise model of hydrophone

Figure A2 shows E_{ni} for various sensor capacitances C_s, with all other circuit values constant as given in Table A1. The effect of impedance is exhibited where the input noise is decreased by 6 dB as the source capacitance is doubled. Note the K and the low-frequency rolloff associated with a high-impedance source. For example, with C_s = 20 pF and f = 10 Hz, the output noise will be down by −10.8 dB (K from Table A2), where

$$E_{no}\ (\mathrm{dB}) = E_{ni}\ (\mathrm{dB}) + K(\mathrm{dB}). \qquad \text{(A2)}$$

Table A2 – Values of K as a Function of Sensor Capacitance C_s for Fig. A2

C_s (pF)	K (dB)			
	10 Hz	50 Hz	100 Hz	20 kHz
20	-10.8	-8.1	-8.0	-8.0
40	-6.5	-4.9	-4.9	-4.9
80	-3.5	-2.8	-2.8	-2.8
100	-2 8	-2.3	-2.3	-2.3
200	-1.4	-1.2	-1.2	-1.2
500	-0.5	-0.5	-0.5	-0.5
1000	-0.3	-0.3	-0.3	-0.3

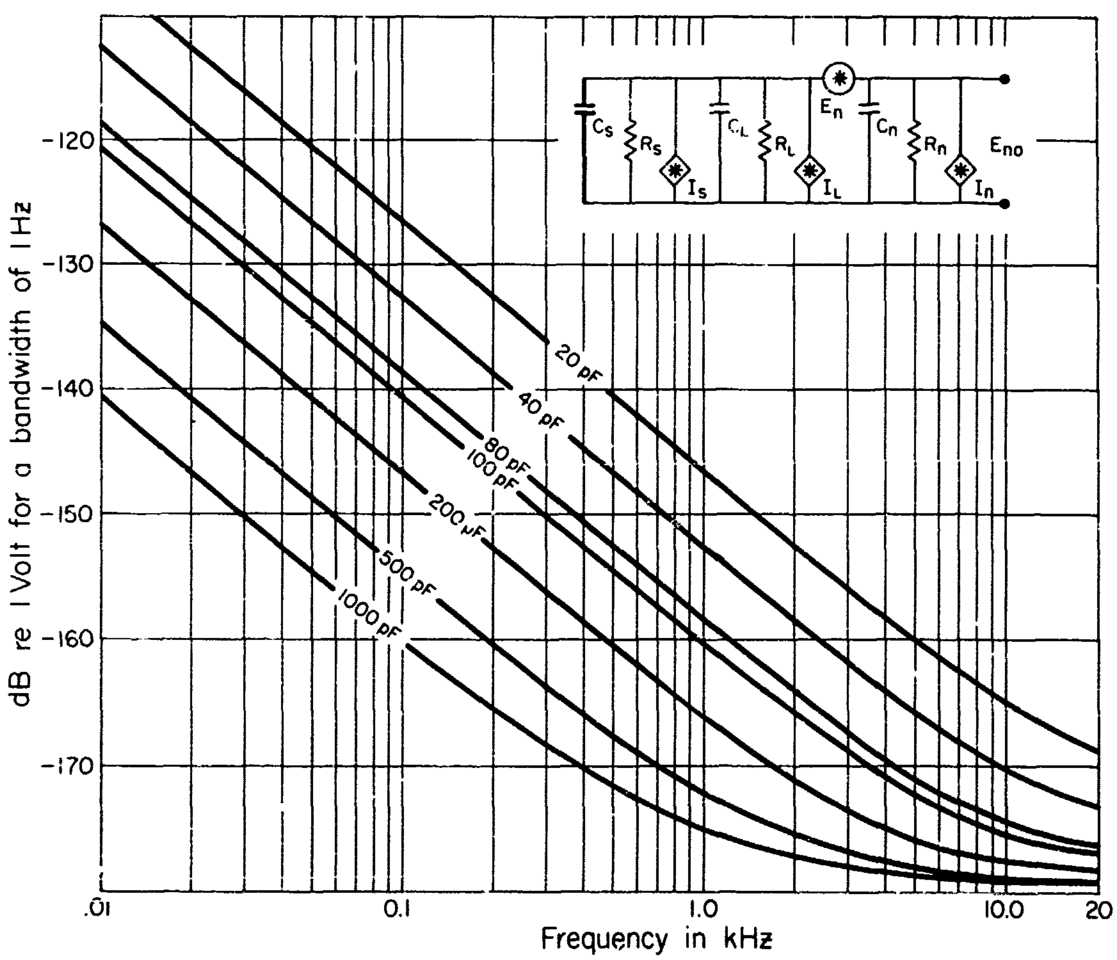

Fig. A2 – Equivalent noise input as a function of C_s

Figure A3 presents E_{ni} as a function of shunt capacitance C_L, with other component values as given in Table A1. E_{ni} is not affected by C_L at low frequencies; however E_{no} is significantly influenced by the increase in K, as indicated by Eq. (A2) and Table A3. Note that

$$K(\text{dB}) \approx 20 \log \left[C_s/(C_s + C_L + C_n)\right]. \tag{A3}$$

Equation A3 is true where the values of K are constant with increasing frequency.

Table A3 gives the insertion loss K that occurs between a low-capacitance sensor element (C_s) and the hydrophone preamplifier input impedance. Circuit designers are often unwittingly influenced by K when they design a preamplifier to have some specific gain, say 10 dB, with the input to the preamplifier short-circuited. This action usually loads the preamp by the input-coupling capacitor, which is usually several thousand picofarads. However, when the

Table A3 – Values of K as a Function of Shunt Capacitance C_L for Figure A3

C_L	K (dB)			
(pF)	10 Hz	50 Hz	100 Hz	20 kHz
20	-3.4	-3.0	-2.9	-2.9
30	-3.9	-3.5	-3.5	-3.5
60	-5.4	-5.1	-5.1	-5.1
100	-7.1	-6.9	-6.9	-6.9
200	-10.2	-10.1	-10.0	-10.0

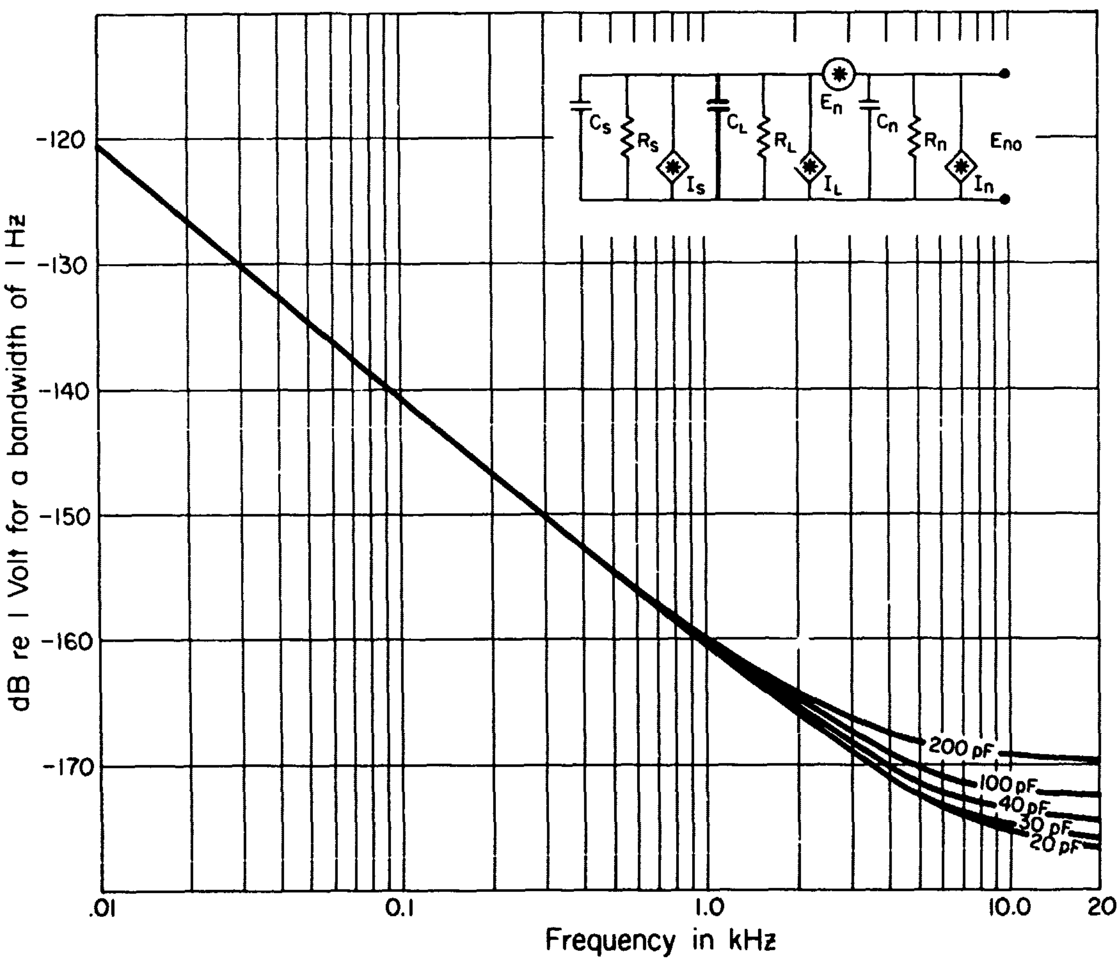

Fig. A3 – Equivalent noise input as a function of C_L

preamplifier is used with a high-impedance source, the preamplifier gain drops to 7 or 8 dB, because the input coupling capacitor and the high-impedance sensor are in series and the preamplifier sees only the sensor. The insertion loss incurred is K.

Figure A4 displays the effect of input capacitance C_n on E_{ni}, with all other circuit values as given in Table A1. The figure shows that the input capacitance has little effect on the equivalent input noise. However, for a very high impedance sensor, K should be carefully observed, because the input capacitance is added to C_L, and the sum in relation to C_s can cause K to become quite large. K can be approximated by

$$K(\text{dB}) \approx 20 \log [C_s/(C_s + C_L + C_n)]. \quad \text{(A4)}$$

Values of K for Fig. A4 are given in Table A4.

Table A4 – Values of K as a Function of Input Capacitance C_n as Given in Fig. A4

C_n (pF)	K (dB)		
	10 Hz	50 Hz	20 kHz
5	-1.9	-1.2	-1.2
10	-2.2	-1.6	-1.6
15	-2.5	-1.9	-1.9
30	-3.4	-3.0	-3.0
40	-4.0	-3.5	-3.5

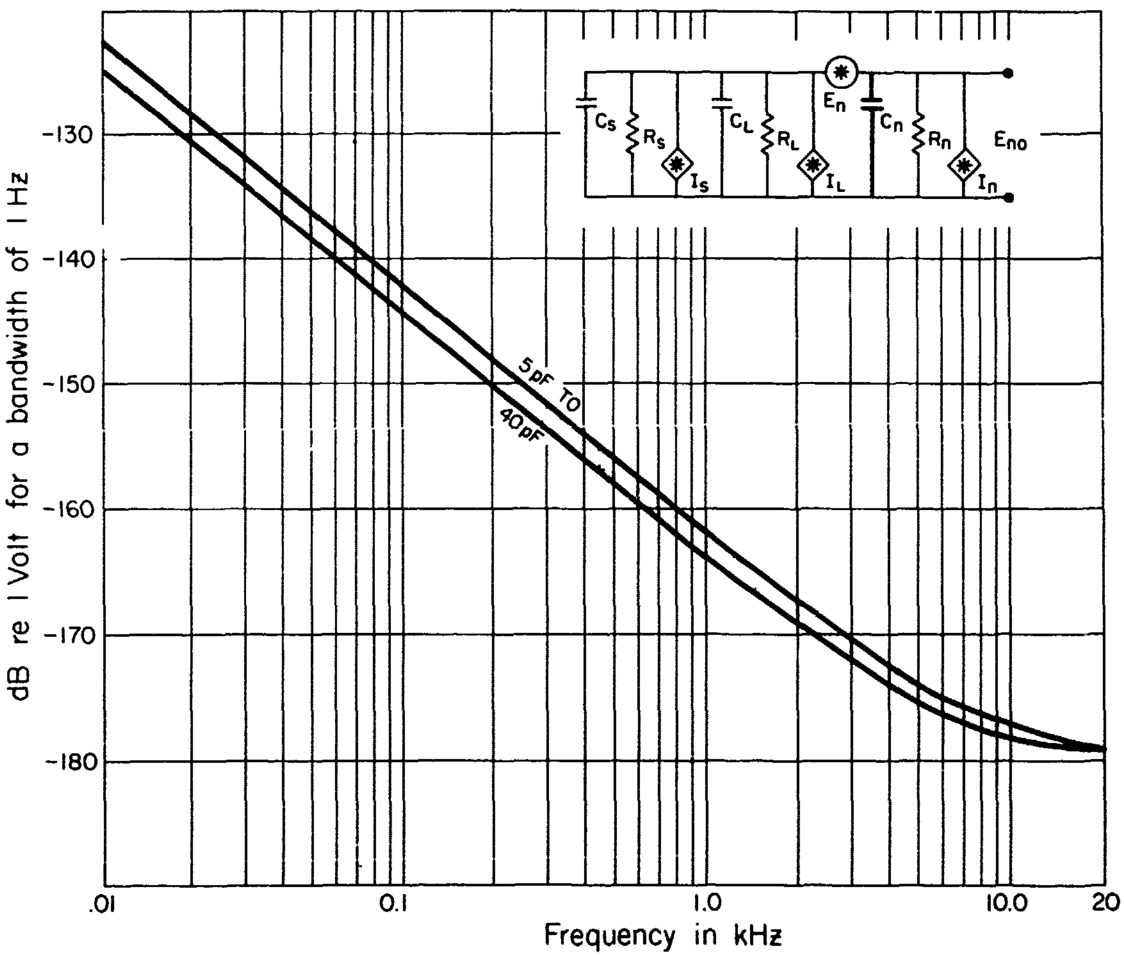

Fig. A4 – Equivalent noise input as a function of C_n

Figure A5 shows E_{ni} as a function of sensor resistance R_s, with other circuit values as given in Table A1. With the constant values selected, E_{ni} is greatly influenced as R_s becomes less than 10^9 ohms. Consequently there are high values of K (Table A5) at low frequencies, where the value of K is determined by the RC combinations across the input of the preamplifier. The break frequency (−3 dB down) is

$$f_{-3\text{dB}} = \frac{1}{2\pi R_T C_T}, \quad \text{(A5)}$$

where

$$R_T = \frac{1}{\frac{1}{R_s} + \frac{1}{R_L} + \frac{1}{R_n}} \quad \text{(A6)}$$

and

$$C_T = C_s + C_L + C_n. \quad \text{(A7)}$$

Table A5 – Values of K as a Function of Sensor Resistance R_s for the Curves Shown in Fig. A5

R_s (Ω)	K (dB)					
	10 Hz	50 Hz	100 Hz	500 Hz	1 kHz	20 kHz
10^7	-24.2	-10.9	-6.4	-2.5	-2.4	-2.3
10^8	-7.3	-2.6	-2.4	-2.3	-2.3	-2.3
10^9	-2.8	-2.3	-2.3	-2.3	-2.3	-2.3
10^{10}	-2.6	-2.3	-2.3	-2.3	-2.3	-2.3
10^{11}	-2.5	-2.3	-2.3	-2.3	-2.3	-2.3

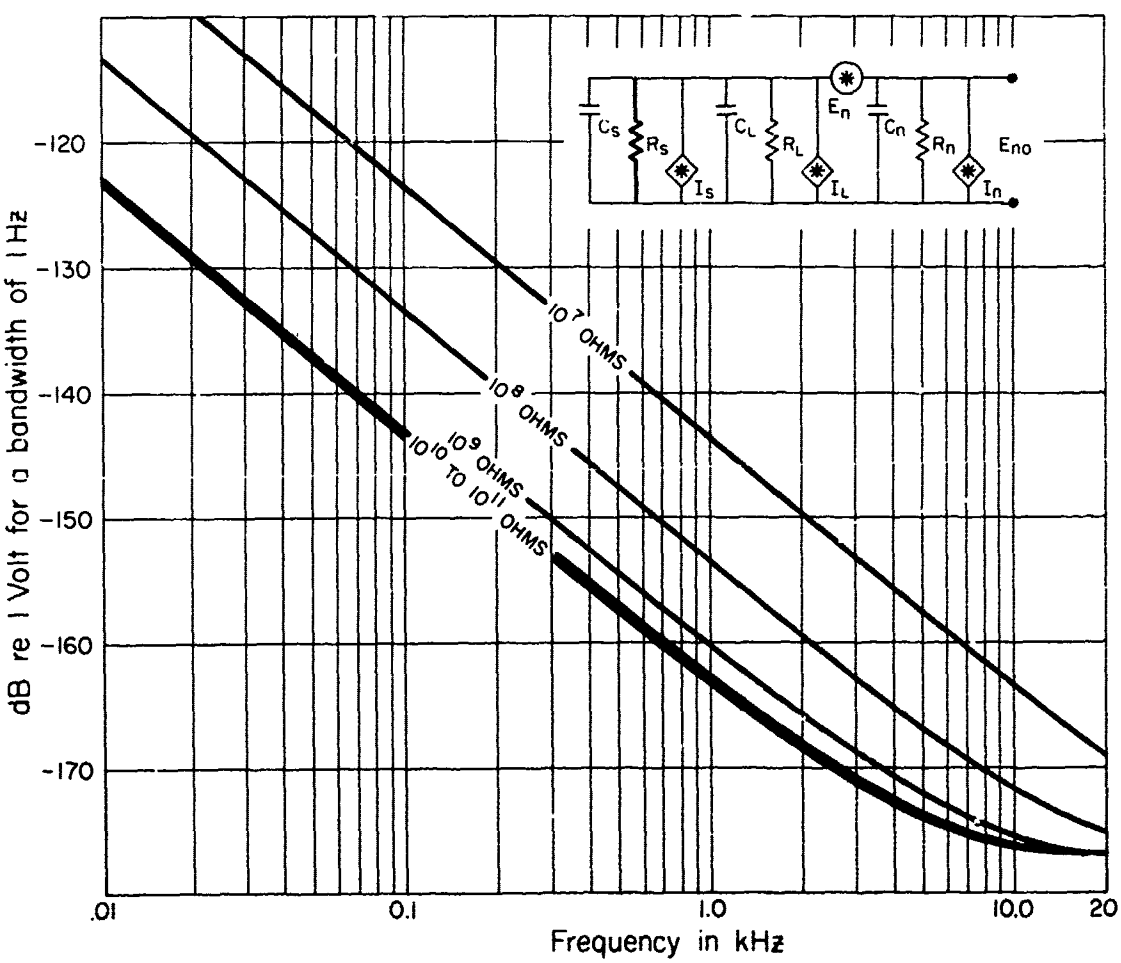

Fig. A5 – Equivalent noise input as a function of R_s

In most hydrophone designs, R_s and R_L are one or two orders of magnitude greater than R_n; also C_L and C_n are less than C_s such that

$$f_{3dB} \simeq \frac{1}{2\pi R_n C_s}. \tag{A8}$$

The variation of E_{ni} and E_{no} with R_L is shown in Figs. A6 and A7 respectively. Low values of R_L can be very influential in the low-frequency response of a system with a high-impedance source. The total load across C_s is the parallel combination of R_s and R_L if the input impedance of the preamplifier is at least a factor of 10 greater. Under the given conditions, as the parallel combination of R_s and R_L becomes $< 10^8$ ohms, the low-frequency rolloff of E_{no} becomes pronounced, as observed in Fig. A7. From Figs. A6 and A7, K values can be obtained where

$$K(\text{dB}) = E_{ni}\ (\text{dB}) - E_{no}\ (\text{dB}). \tag{A9}$$

The effects of varying R_n, with all other circuit values as given in Table A1, are plotted in Fig. A8. Values of E_{ni} and E_{no} are shown for $R_n > 10^7$ ohms. As previously described for R_s and R_L, R_n is most influential at low values and low frequencies, especially if its value is equal to or less than R_L or R_s or their parallel combination.

Noise voltage at the input of the preamplifier as a function of E_n is presented in Fig. A9. At this point of a hydrophone design, significant changes in self-noise can be made by careful selection of the input device (Appendixes B and C). For the best low-noise FETs the manufacturers give E_n at 10 Hz and 1 kHz in nV/$\sqrt{\text{Hz}}$. The noise in other devices is often disguised by giving broadband noise or a noise figure which relates to an amplifier with a specific input resistance.

K is constant for all values of E_n; it is determined by the values of the resistive and reactive components of the model.

Figure A10 gives E_{no} as a function of I_n. As with E_n, I_n is input-device dependent, and the designer is given much latitude in device selections. The value of K is also constant, as with E_n.

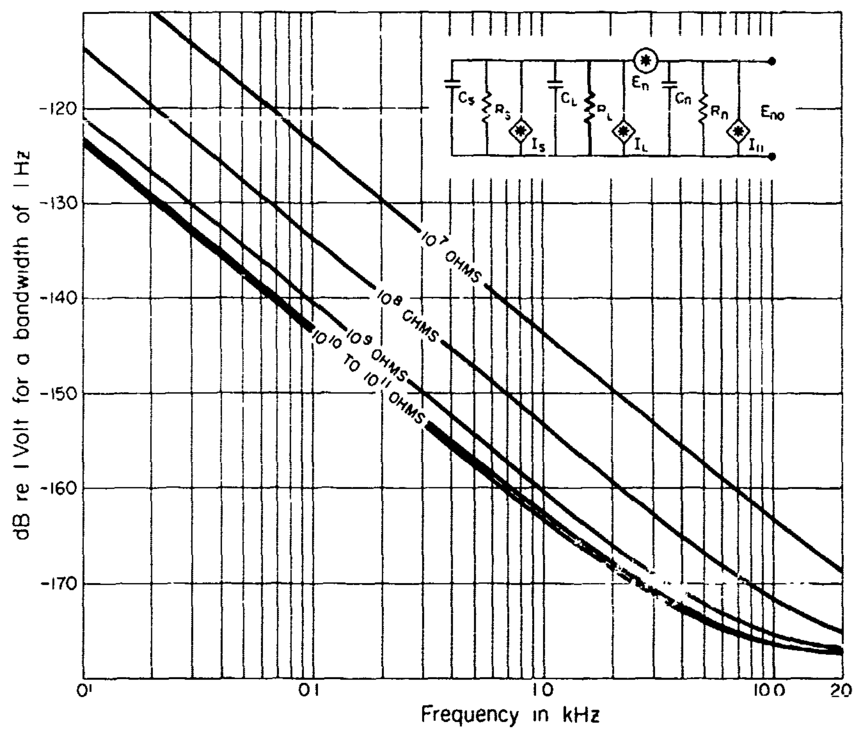

Fig. A6 – Equivalent noise input as a function of R_L

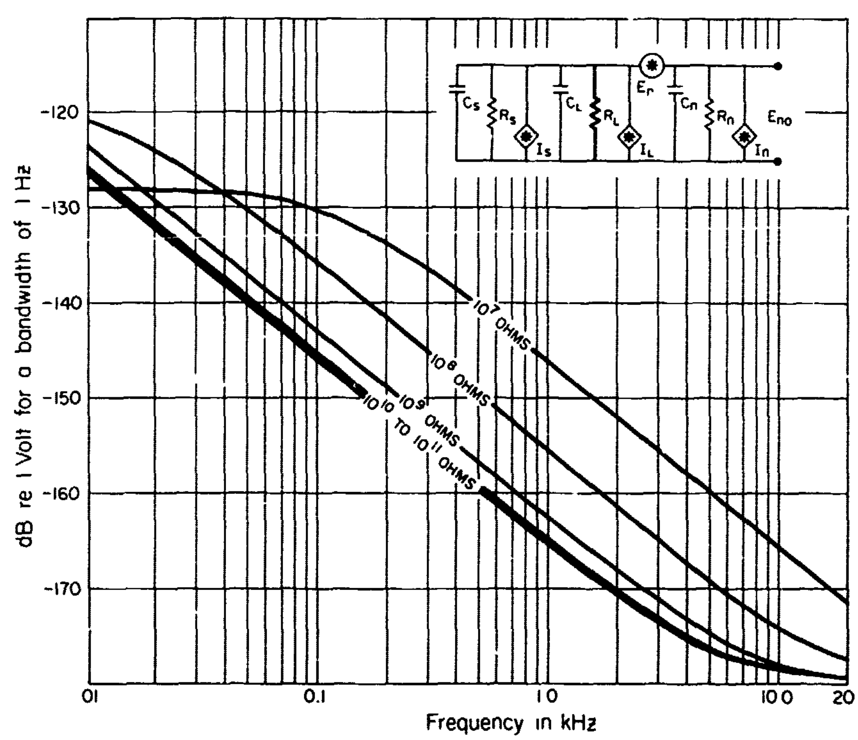

Fig. A7 – Equivalent noise output as a function of R_L

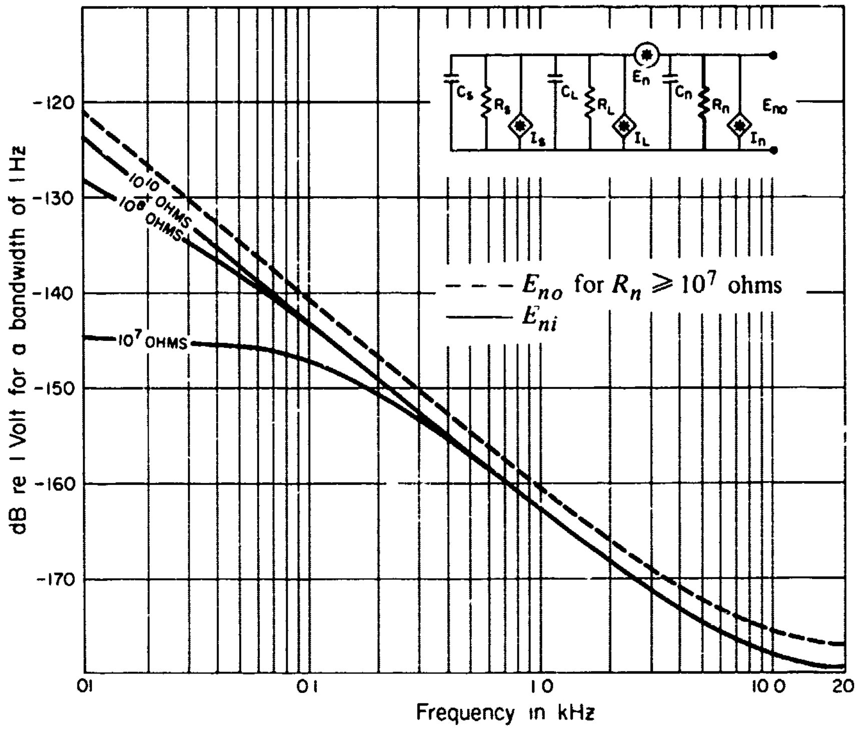

Fig. A8 – Equivalent noise as a function of R_n

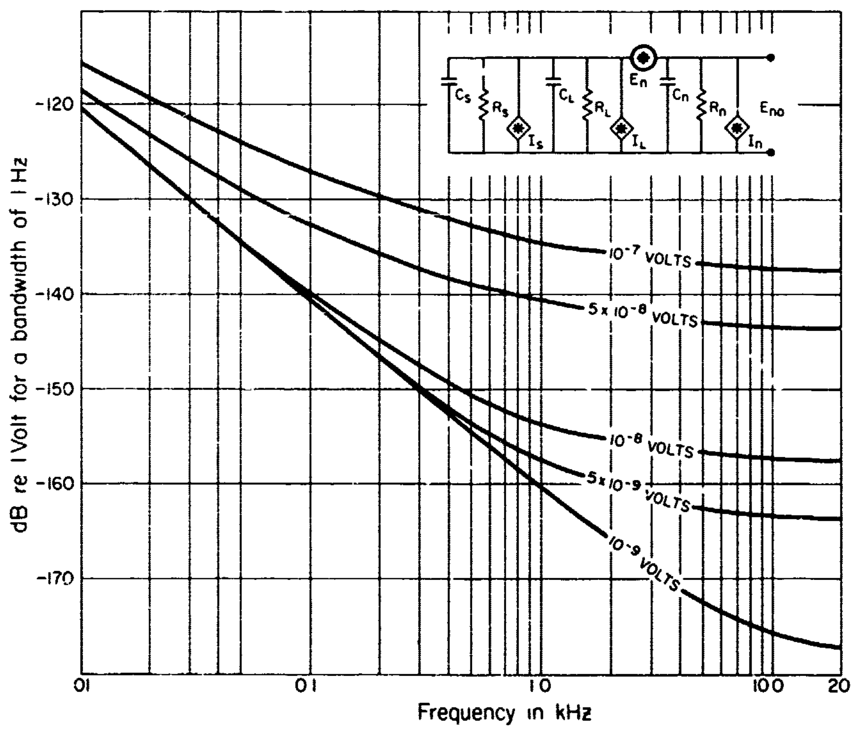

Fig. A9 – Equivalent noise input as a function of E_n

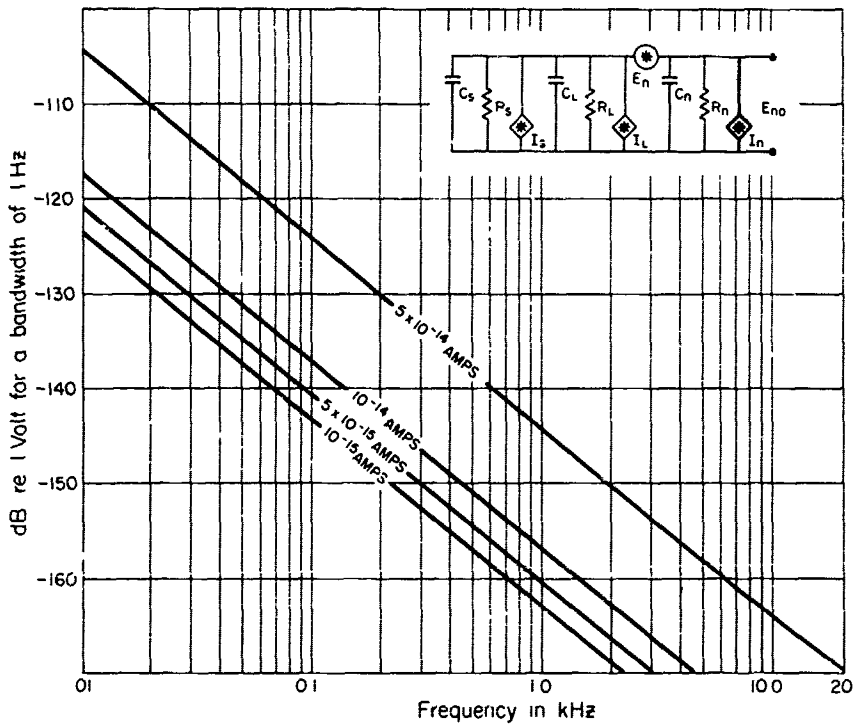

Fig. A10 – Equivalent noise output as a function of I_n

Appendix B

JFETS FOR LOW-NOISE CIRCUIT APPLICATIONS

The JFET is a superior device for hydrophone preamplifier circuits when high input impedance and low self-noise are requirements. Input dc resistance for the JFET can be as high as 10^{13} ohms. The input impedance is the impedance of a reverse-biased PN junction. However, in practice, the impedance is determined by the value of the gate shunt resistor (R_n). When the generator impedance is highly reactive, as in piezoelectric sensors, the JFET is an excellent choice, particularly for infrasonic and audio-frequency applications.

In a low-noise JFET design the equivalent input noise voltage E_n is the significant parameter. On transistor data sheets E_n is usually given as e_n or V_n in nV/$\sqrt{\text{Hz}}$. Noise current is not normally given, because the FET is a voltage-actuated device with noise currents in the region of 10^{-14} to 10^{-15} A/$\sqrt{\text{Hz}}$. However, I_n can be important in low-frequency designs and it can be measured directly or calculated from the gate leakage current [B1, pp. 104-105].

Since E_n and I_n are frequency-dependent parameters, care should be exercised when comparing devices to note the frequency at which they are specified.

Devices are often specified as having a certain noise figure NF or a spot noise figure, instead of using E_n. Care should be taken again when comparing devices, because the NF depends on a specific generator impedance. A high value of generator resistance may make one device appear better than others.

The forward transconductance g_m, or g_{f_s}, and the drain current at zero gate-to-source voltage I_{DSS} are also key parameters for low-noise designs. The transconductance determines the dynamic characteristics of the input circuit and the gain available from the FET. If a high-gain input stage is used, the signal-to-noise ratio can be large enough to negate the noise contributions of subsequent amplifier stages. The noise of the amplifier system will then be

$$E_{no} = E_{ni} A_v, \tag{B1}$$

where A_v is the gain of the total amplifier system.

The g_m is also related to E_n, where E_n is inversely proportional to the square root of the transconductance [B2],

$$E_n \propto 1/g_m^{1/2}; \tag{B2}$$

therefore, as g_m increases, E_n decreases.

To minimize noise, it is necessary to operate the FET where g_m is at its highest value. The highest values of g_m are found at the high values of static drain current I_D, or when I_D is in the vicinity of I_{DSS}, where I_{DSS} is the drain current when the gate-to-source voltage V_{gs} is zero. Operation of the FET at a drain current near I_{DSS} provides superior noise characteristics. Practice has shown that an I_D as low as 0.1 I_{DSS} does not cause a serious increase in E_n [B1, pp. 105-106].

At higher frequencies other transistor parameters, such an input capacitance, become important; however E_n, g_m, and I_{DSS} are the key parameters for low-noise infrasonic and audio-frequency designs.

REFERENCES

[B1] C.D. Motchenbacher and F.C. Fitchen, *Low-Noise Electronic Design*, 1st edition, Wiley, New York, 1973.

[B2] B. Watson, "Audio-Frequency Noise Characteristics of Junction FETs," Application Note AN74-4, Siliconix Inc., Santa Clara, Calif. Aug. 1974, p. 2.

Appendix C
LOW-NOISE HYDROPHONE PREAMPLIFIER

Figure C1 illustrates a typical preamplifier front end used in many low-noise hydrophone designs at the USRD. The common-source, common-collector pair has been used for voltage gains from 10 to 36 dB, with supply voltages from 12 to 48 volts, and with appropriate biasing. The circuit shown has a gain of 20 dB with a supply voltage of from +22 to +34 volts. The most favorable bias conditions occur when V_{cc} is +32 volts.

As stated in Appendix B, optimum low-noise characteristics exist when I_D of the FET is in the vicinity of I_{DSS}. For the preamplifier illustrated, the drain current over the given range of V_{cc} is 0.4 I_{DSS} to 0.9 I_{DSS}, depending on the specific I_{DSS} and pinchoff voltage characteristics of Q2. The nominal value of I_D is about 0.6 I_{DSS} at optimum bias condition (V_{cc} = 32 volts).

The input noise voltage and noise current for Fig. C1 are given in Table C1.

The choice of high-quality, low-noise bias components is essential for consistant low-noise performance of a particular design. Bias resistors for the given circuit are of precision metal-film construction, type RN55, 1% tolerance, MIL-R-10509, except for the gate resistor. Resistor R4 is a high-megohm, thick-film, resistive-glass resistor of 5% tolerance. The input capacitor is a ceramic CK05BX type, MIL-C-11015. The emitter bypass capacitor is a solid-tantalum, established-reliability type, MIL-C-39003.

Table C1 – Input Noise Voltage E_n and Current I_n for Fig. C1

Frequency (Hz)	E_n (V/$\sqrt{\text{Hz}}$)	I_n (A/$\sqrt{\text{Hz}}$)
50	5.6×10^{-8}	2.5×10^{-14}
100	6.7×10^{-9}	2.5×10^{-14}
20 k	5.6×10^{-9}	2.5×10^{-14}

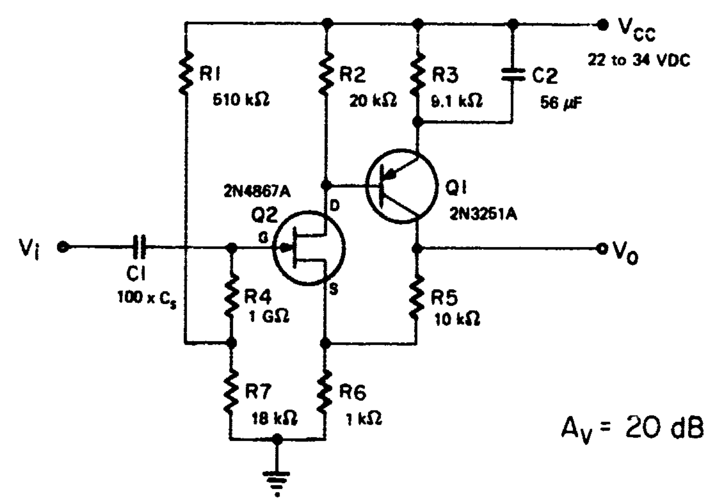

Fig. C1 – Typical USRD-type low-noise amplifier